International Journal of Scientific Engineering and Technology Research

ISSN 2319-8885
Vol.03,Issue.29
October-2014,
Pages:5879-5884

www.ijsetr.com

Optimal Battery Charging in a Solar-Powered Robotic Vehicle with the Solar Tracking Mechanism

K.S.RAJESH KUMAR[1], R.JAYA KUMAR[2]

[1]PG Scholar, Dept of ECE, Vemu Institute of Technology, JNTUA, Chittoor, AP, India, E-mail:ksrajeshkumar1318@gmail.com.
[2]Asst Prof, Dept of ECE, Vemu Institute of Technology, JNTUA, Chittoor, AP, India, E-mail: jayaraji1984@gmail.com.

Abstract: This paper focuses on the design an optimization charging system for solar powered robotic vehicle by means of tracked solar panels. Thus, the implementation of a complete energy management system for the robotic vehicle. This proposed system was tested on the VANTER robotic platform. The smart host microcontroller used to design the proposed system .the proposed system has main two contributions. .one contribution is the solar tracking system for to increase power of the system regard less the mobility. Another one is it proposes an alternative design of power system performance based on a pack of two batteries. The aim is completing the process of charging a battery independently while the other battery provides all the energy consumed by the robotic vehicle.

Keywords: Li–Po Battery, Mechatronic System, Photovoltaic (PV), Robotic Vehicle, Solar Tracker.

I. INTRODUCTION

SOLAR power systems in autonomous robotic vehicles have been often used for some years. A real example is the Sojourner rover, in which most of the supplied energy is generated by a reduced-size photovoltaic (PV) panel [1]. However, in case of scarce to no solar light, the rover should minimize consumption, since its batteries in line could not be recharged when depleted [2]. The use of rechargeable batteries in a space mission was used for the first time in the Mars Exploration Rovers. Nevertheless, the need for greater operation autonomy by Spirit and Opportunity was solved by means of larger deploy solar panels [3]. This solution works as the basis for the design of solar panels for the future ExoMars mission.

Fig.1. VANTER: a solar-powered robotic vehicle.

This rover, thanks to its high-efficiency ultrathin-film silicon cells constructed on carbon-fiber reinforced plastic, is capable of providing higher power [4], [5]. NASA designs inspired different generations of exploration vehicles [6]. This is the example of K9, a rover for remote science exploration and autonomous operation [7]; field integrated design and operations, an advanced-technology prototype by Jet Propulsion Laboratory for long-range mobile planetary science [8]; and Micro5, a series of robotic vehicles devised for lunar exploration [9]. As its main design advantage, this rover series has a dual solar panel system coupled to an assisted suspension mechanism. This prevents the manipulator arm mounted on the middle of the rover from having to minimize solar panel-generated power and allows it to dust solar panel surface.

II. MOBILE ROBOTIC PLATFORM

VANTER—Spanish acronym for autonomous unmanned exploration vehicle specialized in recognition—is a robotic exploration vehicle developed at the rover was developed to be guided and has a set of four wheels coupled to a plane chassis that can rotate independently as shown in Fig.1. The four-wheel-drive (4WD) and the individual control of each wheel allow different types of movement; including Ackerman configuration, the crabbing maneuver or the rotation with inner inertial center. The four wheels in VANTER are sustained by means of independent passive suspension of double aluminum fork to absorb terrain vibrations. Each wheel consists of two motors, one for rotation and another for driving. On the one hand, forward movement is produced by means of dc motors (12 V and 60 mA) that provides 120 r/min with a torque of 8.87 kg/cm. On the other hand, the rotation motor provides a speed of 152 r/min Among others instruments aboard VANTER disposes of a 5-DOF robotic arm, an Omni Vision MC203 wireless

micro camera, and an analog video receiver with a Pinnacle Dazzle DVC100 video capture card [20]. Its reduced weight, small dimensions, and versatility make VANTER suitable as a robotic exploration vehicle.

III. MECHATRONIC SYSTEM DESIGN

A typical power management design consists of smart batteries integrating both communication devices and electronics able to control the charge. However, when an economical system is required, the concept of intelligence should be applied to software design for simple batteries. One of the main objectives of this paper is the implementation of the SHM concept to develop a low-cost power management system aboard a robotic vehicle. The system consists of an electrical circuit interconnecting a PV system, a charger device, a selector system, a batteries monitor system, and a battery system as shown in Fig.2.

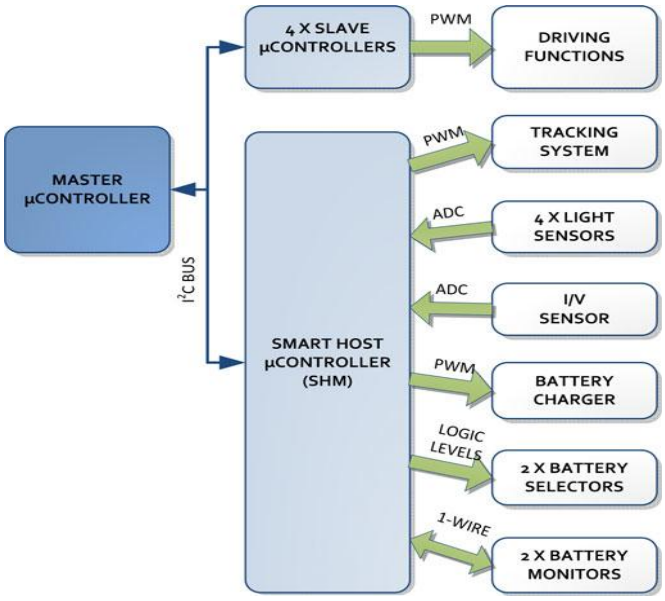

Fig.2. Block diagram of the hardware architecture for VANTER.

A. Photovoltaic System With Solar Tracking Mechanism

When selecting the solar panels, VANTER physiognomy and consumption dictated its construction and electric requirements (see Section IV-C). The panel weight is a factor that limited its mechanical design; light-weight panels provide lower power consumption and require optimizing the robot's overall performance. The proposed PV system consists of three mono crystalline solar panels with laminated PET, whose dimensions are 200 mm × 250 mm × 3.2 mm and its weight is 0.7 kg per panel. The PV system provides power, keeping in mind that voltages and currents generated must adapt to the maximum and minimum values of the hardware. However, since the environmental natural features cannot be predicted at each instant, the quantitative energy from solar radiation cannot be predicted either. Thus, one of the main proposals of this paper is the implementation of a solar tracking mechanism aimed at increasing power levels in the PV panels. Unlike other rovers that use navigation techniques to guide their panels toward the Sun [12], VANTER's mobility does not represent a disadvantage, since the proposed tracker system looks for the most powerful light source.

Solar tracker prototypes built in mobile robots have proven that orientation of PV systems leads to increased energy efficiency relative to systems with fixed solar panels (20–50% per collector) [23]. This gain depends on several construction strategies of the solar tracker such as the type of axis movement (either single or dual), type of sensors on which is based (photoresistors or photoconductive cells), and the accuracy rendered by the number of sensor pairs [24]–[26]. On the contrary, parasitic load consumption associated to the proposed configuration (a mobile solar panel, two batteries, and electronics) compared to a simple system (a fixed panel, a battery, and electronics) is increased between 1.14% and 21.42%. The consumption increment varies mainly due to the operation of the solar tracking system, which is based on servos; thus, standard dc motors is proposed to reduce the consumption up to 8.57% as shown in Fig.3.

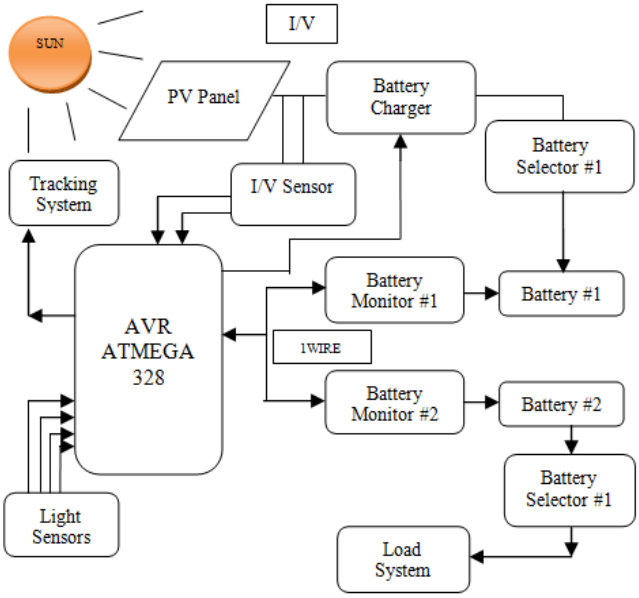

Fig.3. Overall scheme of the power management system of VANTER.

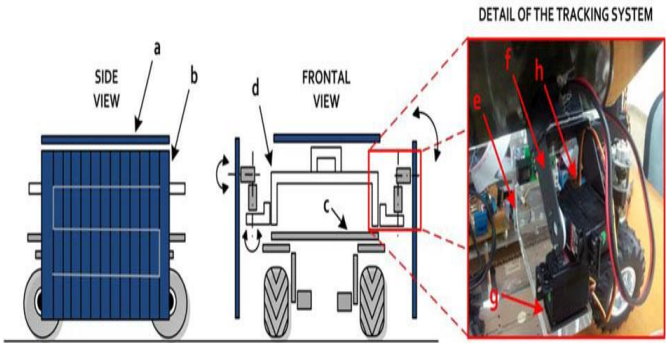

Fig.4. Mechanical design of the solar tracking system of VANTER: (a) upper solar panel, (b) mobile solar panels, (c) aluminum chassis, (d) metha crylate chassis, (e) methacrylate support, (f) pan and tilt unit, (g) pitch servomotor, and (h) yaw servomotor.

The tracking system design is based on solar-type CdS photoconductive cells. This consists of four Hamamatsu S9648-100 photosensors mounted on a PCB attached to one solar panel of VANTER (see Fig.4). The advantage of the selected devices is that they have a spectral sensitivity peak near 600 nm where light is considered to have more energy. To improve the performance of the tracking system, the photoconductive cells are arranged in a crosspiece and their field of vision is narrowed by means of opaque plastic tubes with an outwardly directed gap. Thus, this system provides a method to determine the brightness value at each cardinal point regarding the plane of the solar panel. The advantage over other systems based on solar mathematical equations is that this mechanism allows tracking as closely as possible to the solar position in any ambient light situation [23]. To this end, PCB allows calibrating photo sensors' sensibility by means of variable resistors, which has the advantage of adapting to different brightness locations and lighting conditions.

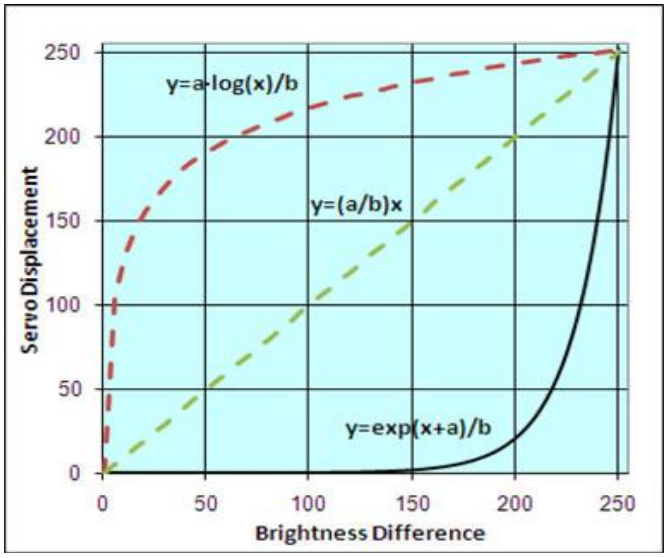

Fig.5. Graphical representation of different servo control signals: equation implemented (continuous line) and other equations studied (dashed line).

Tracking the most powerful light source is possible because analog signals are obtained by the photo sensors since they already include both amplifier and signal conditioner integrated circuits. Proportional light values are compared in pairs and, from their difference, adjusting the control signal for azimuth and elevation required by the tracking system. Each servo is controlled by a pulse width modulation (PWM), whose duty cycle determines the required rotation. Instead of increasing or decreasing the duty cycle at fixed values until servos face the light source, rotations are achieved by means of PWM signals generated as shown in Fig.5. This mathematical expression responds to an SHM programmed algorithm where **y** stands for servo displacement, x is the difference of illumination between each couple of photo sensors, and constants are values experimentally obtained in ground testing (see Fig.5). The advantage of this strategy relative to other types of equations (i.e., linear or logarithmic) is the servos performing large displacements when the lighting values between each pair of photo sensors evince high discrepancies on its axis. Similarly, shorter and accurate shifts are obtained when lighting values are approaching the most powerful light source. In this way, the pan and tilt units try to place mobile solar panels perpendicularly to the most intense light source available. Higher energy collection is therefore possible. On the other hand, the tracking algorithm also takes into account VANTER's kinematics configuration. Thus, it prevents servomotors from reaching limit positions during rotation so as to prevent solar panel from colliding with other robotic elements.

B. Batteries Switching System

The switching system consists of two MAX1538EVKIT selectors with break-before-make operation logic. Their function is connecting electrically the charge and discharge paths between the batteries, the charger module, and the load system (see Fig.6 and 7). That is, selector 1 is inserted between the charger and the dual-battery pack. Its function is routing the current from the PV panels to the input of the charger and, from there, to the battery selected in each moment. Selector 2 is used to connect the selected battery to the load system. Therefore, the dynamic connections of the electric circuit are carried out according to the SHM-defined logical operation mode. This is based on the voltage thresholds programmed into the control algorithm.

C. Charging and Discharging System

When describing the implemented system, two different parts can be distinguished: a first one exclusively devoted to the intelligent management of the charging/discharging process, including controlling and monitoring sensor signals, and a logical part devoted to power flow management through VANTER energy sources. MAX17005BEVKIT was the charger system used. This device consists of a dc–dc synchronous-rectified converter with step-down topology (efficiency over 90%) (see Fig. 8). The charger system is controlled by the SHM using a PWM signal applied to one of its terminals and supplies each battery according to a programmed algorithm. Between the PV system and the charger system there are a voltage conditioning capacitor and an I/V sensor from AttoPilot with 0–3.3 V output. The capacitor C1 prevents voltage at the charger input pin V_{ch} from falling below the charge voltage of the battery cells V_{cv} when solar power is not capable of providing appropriate voltage level Vs. During that instant the capacitor is discharged with a current I_{ch} through the dc–dc converter. The role of the I/V sensor is detecting the current and voltage levels that solar panels provide to the charger device.

The algorithm implemented in the SHM consists of a charge regulation by increasing the output current of the charger module according to the MPP. The MPP-tracking scheme is based on the dynamic power path management (DPPM) function described by Texas Instruments

Incorporated [27]. This low-cost solution is a simplified MPP tracker able to harness 90–95% of maximum power. On this basis, a voltage variation in the PVpanels is detected by the I/V sensor as a power variation.

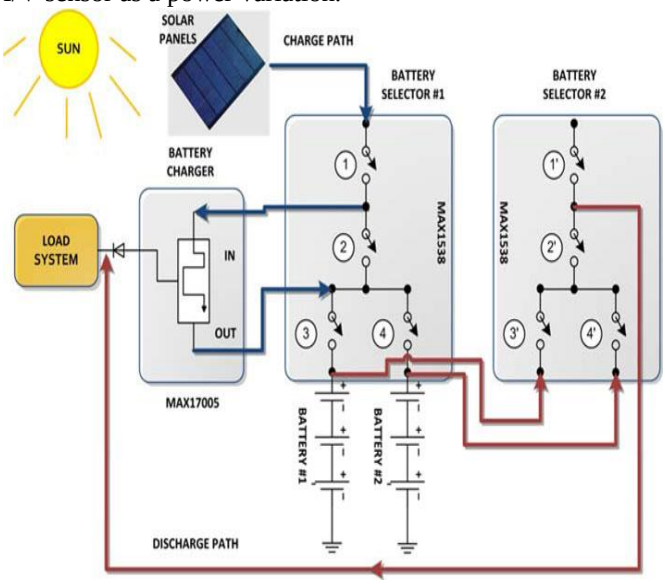

Fig.6. Overall connection diagram for batteries selectors.

The logical operation for charging and discharging modes is shown in Table I.

D. Batteries Monitoring System

The aim of the monitoring system is maximizing the life and energy storage of Li–Po cells. Therefore, the main function of this system is monitoring the state of charge (SoC) of the batteries and accurate control of the charging–discharging cycles. The use of a dual battery monitor system was required for control and parameter measurement. This module consists of two DS2788EVKIT+ integrated circuits manufactured by Maxim- IC. Each of these is connected to the batteries in parallel—so that the charge/discharge current passes through its measuring resistor—and by means of a 1-Wire bus multi drop type, both to the load system and the charger through the SHM. The main advantage of the dual monitoring system is that it allows continuous measurement of both the capacity of the battery in charge as well as of the one being discharged. Among other essential monitored parameters such as voltage, current, and temperature—which prevent batteries from working near their warming limits—the monitor displays some other important parameters such as the batteries' SoC, relative capacity (%), absolute capacity (mAh), state of health (SoH), and internal resistor (Rint).

TABLE I: Logical Operation Mode of the Battery Selectors

Battery Selector	1	2	3	4	1'	2'	3'	4'
#1 Charging & #2 Discharging	C	O	C	O	X	C	O	C
#1 Discharging & #2 Charging	C	O	O	C	X	C	C	O

C = Closed, O = Open, X = No Connected

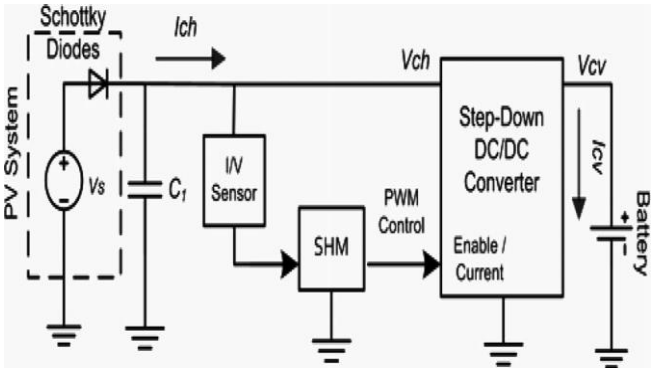

Fig.7. Connection diagram of the charger system.

E. Rechargeable Battery System

The design implemented in this paper proposes the use of two separate battery units working alternately [see Fig. 8(a)]. Thus, one of the batteries receives the charge current from the PV system while the other provides VANTER with all the energy it requires. Unlike other designs, in a conventional system the power source is used to recharge a single battery [see Fig. 8(b)]. As a disadvantage, the robot can only be used when the battery is fully charged and must remain idle during the recharging.

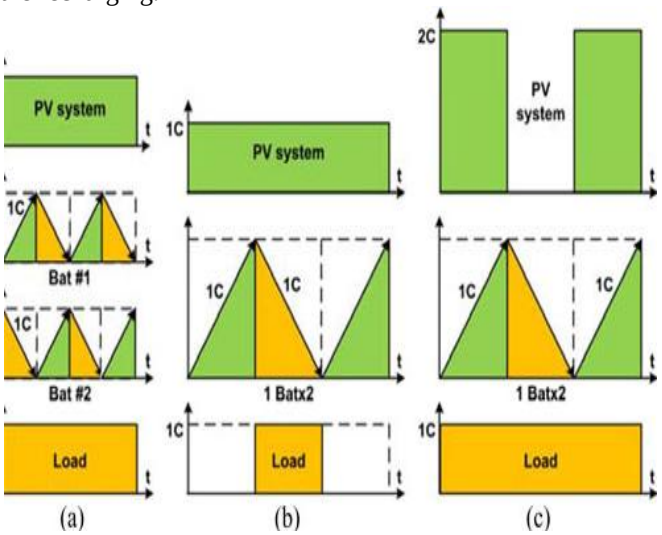

Fig.8.Different strategies of solar-powered robots with battery system: (a) dual battery system, (b) conventional system, and (c) load sharing system.

IV. POWER SYSTEM DESIGN

This section presents the sizing of the batteries system, the parameterization of the charging and discharging algorithm, and the sizing of the PV system in more detail.

A. Batteries Sizing

Each battery was sized taking into account both the maximum system consumption and VANTER continuous consumption under different operation conditions (see Table III). It should be also guaranteed that maximum system consumption is always below the maximum battery-deliverable discharge. Nevertheless, an Li–Po battery working at its maximum continuous discharge has the disadvantage of not providing the required performance and shortening its lifetime (e.g., 80% of capacity for 500 cycles at

10 C). Thus, keeping in mind that the selected batteries deliver peak currents of 23 C (over 55 A) and sustain a continuous consumption of 15 C (36 A), VANTER consumption requirement is fully covered. Thus, setting the required backup time, the capacity of each battery can be estimated by means of the following formula:

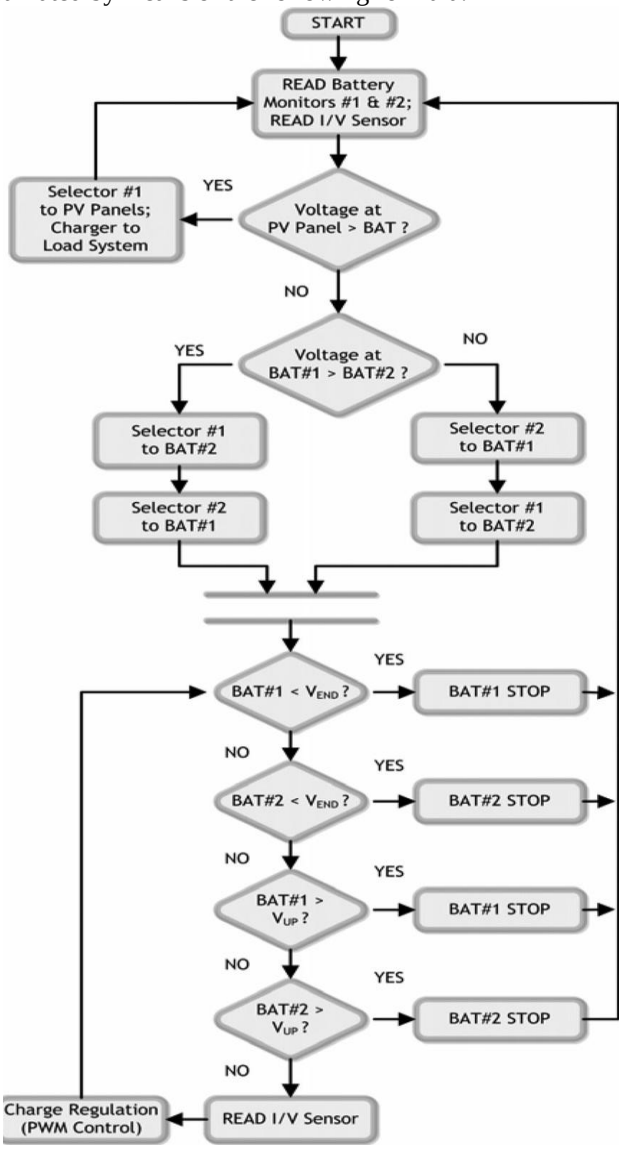

Fig 9: Algorithm of the charging and discharging cycle.

$$\text{Capacity (mAh)} = \text{ton(min)} \times \text{Current demand (mA)} 60\text{min/h} \quad \textbf{(1)}$$

B. Charge and Discharge Parameterization

On the other hand, threshold values for the dynamic charging/discharging regulation were defined in the SHM programmed algorithm to prevent Li–Po batteries from damaging and to extend their life cycle (see Fig.9). The charging and discharging process parameterization has been set considering he battery electrical model, where the battery stands for a voltage source with an internal resistor in series Rint specified by the manufacturer. Considering the voltage drop across the battery(Vint = 0.3 V) and a cutoff voltage Vcutoff for the charging and discharging algorithm, a maximum and minimum voltageVup and Vend were defined for the charging and discharging protection conditions. V).

C. Sizing of the Photovoltaic System

The power requirement of the PV system results from the estimation of the voltage and current values that the charger supplies to the battery (see Fig.10). The maximum voltage at the charger output corresponds to the voltage of the fully charged battery during voltage regulation, which in this case corresponds to Voc = 12.6 V. In a dc–dc converter with step-down topology a voltage higher than 12.6 V is required at the input, so the PV panel voltage at the MPP must exceed this value. Besides, each battery employs a capacity of 2400 mAh, its charge being advisable at a rate between 0.2 and 0.7 C. This corresponds to a charge current between 480 and 1680 mA, with an intermediate value of 0.5 C (1200 mA) a relatively good choice. There by according to these considerations, the power required by the PV system is

$$Ps = Pschottky + (Pbat/Efficiency) \quad \textbf{(2)}$$

Where Pschottky is the power loss across the Schottky diodes that protect the PV panels, Pbat is the power delivered to the battery in the charging process considering 90% charger efficiency, according to the manufacturer. As a result, it is obtained that Ps = 16.56 W. Assuming Ps tolerance is within 10%, power requirement is covered with a set of three PET panels as those chosen according to the manufacturing specification (VMPP = 14 V, IMPP = 430mA, and Pmax = 6 W). In short, it complies that Pmax · n > (Ps± 0.1 Ps), where n stands for the three solar panels electrically connected in parallel to comprise the PV system.

V. RESULTS

In different lightning conditions no of tests are performed on the solar panels to access the power generations. Battery system working is understood by the charging and discharging the charging and discharging operation proposed

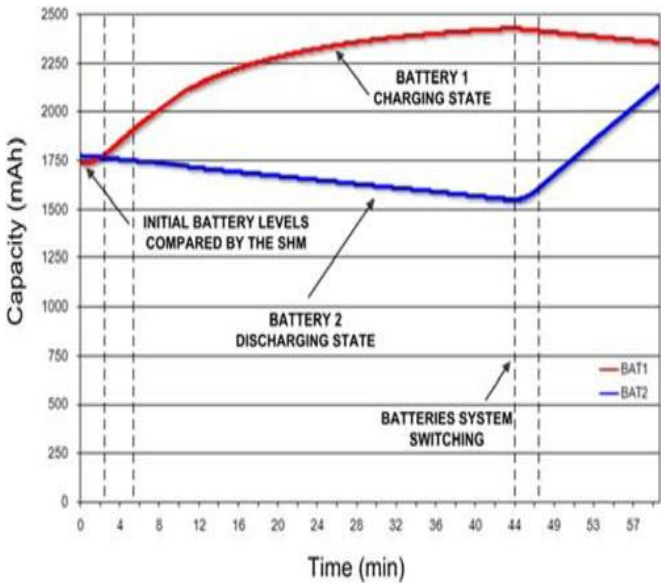

Fig.10. Capacity curves in the batteries for a charging and discharging cycle.

in this paper. The capacity stored and delivered to the load system in terms of power during the charging and discharging states is shown in Fig. . Initially, the algorithm of the SHM detects the battery with lower capacity and carries out its charging while the battery with higher capacity supplies the load system In summary, the constant-current charging phase—in which the Li–Po battery is considered charged to a75–80%—takes up relatively short time, while the following phase (80% to 95–100%) takes much longer as shown.

The proposed system can communicates with the Zigbee wireless module the optimal solar tracking robotic vehicle can also sense the temperature and detect the obstacles send the information to the PC through wireless Zigbee module and result is displayed on the PC as shown in Fig.11.

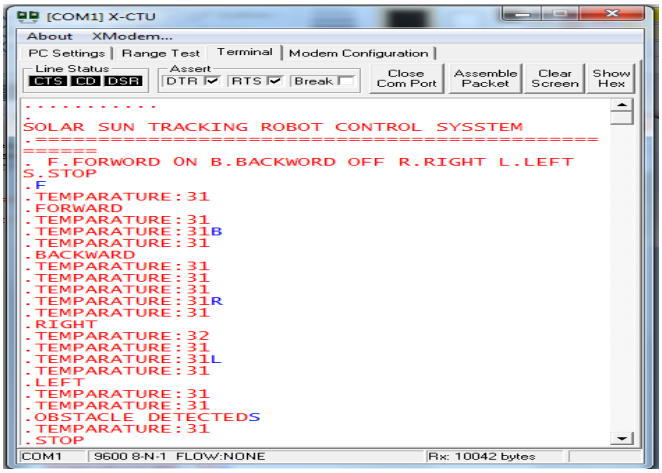

Fig.11. Result displayed on the PC.

VI. CONCLUSION

This paper has presented optimization of battery charging in solar vehicles which gives the a smart energy management system applied to a solar robotic platform called VANTER the proposed system is aimed to increase the system energy by the use of the solar tracking mechanism, which increase the power regard less the mobility of the mobility of the vehicle. By implementing a dual system of selectors, monitors, and batteries. The proposed mechanism is capable of tracking maximum light intensity. the systems' energy requirements recharging the backup battery were made possible This strategy implies small solar panels to power a single battery at a time. Good relation between total weight, capacity available, and source-required power is reached. An SHM was designed for optimal charge regulation by means of an MPP tracking scheme based on the DPPM. Experimentation shows that the charging and discharging processes that require careful Li–Po cells became possible due to a fine SHM-implemented control algorithm.

VII. REFERENCES

[1] D. L. Shirley, "Mars pathfinder microrover flight experiment. A paradigm for very low-cost spacecraft," Acta Astronaut., vol. 35, pp. 355– 365, 1995.

[2] H. J. Eisen, L. C.Wen, G. Hickey, and D. F. Braun, "Sojourner mars rover thermal perfomance," presented at the 28th Int. Conf. on Environmental Systems, Danvers, MA, 1998.

[3] Stefano, B. V. Ratnakumar,M. C. Smart, G. Halpert, A. Kindler, H. Frank, S. Di, R. Ewell, and S. Surampudi, "Lithium batteries on 2003 mars exploration rover," presented at the IEEE 17thAnnu. Battery Conf.Applications and Advances, Long Beach, CA, pp. 47–51, 2002.

[4] M. Bajracharya, M. W. Maimone, and D. Helmick, "Autonomy for mars rovers: Past, present, and future," Computer, vol. 41, no. 12, pp. 44–50, 2008.

[5] A. K. Baluch, "Re-use of exomars rover on icy moons of jupiter," M.Sc. thesis, Dept. Space Sci., Crandfield Univ., Swindon, U.K., 2010.

[6] The Rover Team, "The ExoMars rover and Pasteur payload Phase a study: An approach to experimental astrobiology," Int. J. Astrobiol., vol. 5, no. 3, pp. 221–241, 2006.

[7] J. L. Bresina, M. G. Bualat, L. J. Edwards, R. J. Washington, and A. R. Wright, "K9 operation in May '00 dual-rover field experiment," presented at the 6th Int. Symp. Artificial Intelligence, Robotics and Automation in Space, Montreal, QC, Canada, 2001.

[8] P. S. Schenker, E. T. Baumgartner, P. G. Backes, H. Aghazarian, L. I. Dorsky, J. S. Norris, T. L. Huntsberger, Y. Cheng, A. Trebi-Ollennu, M. S. Garrett, B. A. Kennedy, and A. J. Ganino, "FIDO: A field integrated design & operations rover for mars surface exploration," presented at the 6th Int. Symp. Artificial Intelligence, Robotics and Automation in Space, Quebec, QC, Canada, 2001.

[9] T. Kubota, Y. Kunii, Y. Kuroda, and M. Otsuki, "Japanese rover test-bed for lunar exploration," in Proc. Int. Symp. Artif. Intell., Robot. Automat. Space, no.77, 2008.

[10] M. S. Schneider, A. Bertrand, R. Lamon, P. Siegwart, R. vanWinnendael, and A. Schiele, "SOLERO: Solar powered exploration rover," presented at the 7th ESAWorkshop Advanced Space Technologies for Robotics and Automation, Noordwijk, The Netherlands, 2002.